

Multi-physics Coupling Simulation of Heat Transfer and Thermal Design for High Voltage Switchgear Busbar Room

Wei Zheng^a, Wenrong Si^b, Chenzhao Fu^b, Dengfeng Ju^c, Chuan Chen^c, Sen Qian^c, Jian Yang^{a,*}, Qiuwang Wang^a

^aMOE Key Laboratory of Thermo-Fluid Science and Engineering, Xi'an Jiaotong University, Xi'an 710049, China

^bState Grid Shanghai Electrical Power Research Institute, Shanghai 200437, China

^cGlobal Energy Interconnection Research Institute Co. Ltd., Beijing 102209, China
 yangjian81@mail.xjtu.edu.cn

High voltage, heavy current, miniaturisation and long service life are the current development trend of high voltage switchgear, which would require high heat dissipation performance for the switchgear. In the present paper, based on the finite element method, the heat transfer in the busbar room of KYN28A high voltage switchgear is numerically studied using the electromagnetic-heat-flow coupling model. The heat dissipation performance in the busbar room under natural convection, forced convection, and using a heat pipe are discussed. Firstly, it is found that natural convection alone cannot meet the demand of increasing the current carrying capacity of switchgear. The temperature rise of the contact inside the contact box is higher than 65 °C, which cannot meet the IEEE standard. Secondly, with the forced convection method, the optimal working flow rate of double groups of a fan is 1.5 m/s, and that of a single group of a fan is 2 m/s. With the same inlet air velocity, the heat dissipation performance is better by using double group fans. Finally, it is found that the overheating problem of the contact system can be solved effectively when the fans are combined with heat pipe, and the heat dissipation performance in the busbar room would be good with low inlet air velocity.

1. Introduction

High voltage switchgear plays the role of on-off, control or protection in power generation, transmission, distribution, power conversion and consumption of the power system. The development of switchgear towards high voltage, heavy current, miniaturisation and longevity. The development trend will not only increase the heating power but also weakens the heat dispersion of the switchgear. Therefore, the current development trend of switchgear puts forward more efficient heat dissipation measures.

Scholars from home and abroad have done a lot of research about the temperature rise of switchgear and its influencing factors through simulation or experiment and put forward the corresponding heat dissipation measures. Li et al. (2019) studied the influence of load current, contact resistance and ambient temperature on the temperature rise of switchgear. Szulborski et al. (2021) applied the insulator made of halogen-free polyester fireproof material, which greatly improved the heat resistance of low-voltage switchgear. Ruan et al. (2019) studied the optimisation method of numerical calculation of heat-flow field inside switchgear from three aspects: grid optimisation, external boundary conditions of switchgear and heat source of the internal component. Forming different forced convection conditions in the switchgear by setting different groups of fans and fans fault status, Wang et al. (2021) analysed the temperature rise in the switchgear under corresponding conditions. Bedkowski et al. (2016) used a genetic algorithm to optimise the switchgear busbar system: the weight of the bus system is reduced by 4.5 %, and the average temperature rise of the bus is about 2 - 3 K. Bedkowski et al. (2017) adopted heat dissipation measures including changing the surface emissivity of busbar, changing the inlet and outlet grids of switchgear and radiator to reduce the temperature rise of switchgear. Jia et al. (2020) improve the accuracy of temperature rise and position of hot spot inside the 400 kVA oil-immersed transformer by the method of multi-physical field coupling. Guan et al. (2015) analysed the electrical, thermal and mechanical behaviour of the plug-in connectors of Gas Insulated Switchgear under steady-state and short-circuited

conditions. Liu et al. (2019) studied the influence of the shape of the heat pipe's adiabatic section, evaporation section and ventilation area of different parts of the switchgear on the cooling effect of the contacts system through experiment. Wang et al. (2020) studied the temperature rise characteristics under different current values, phase imbalance, different ventilation conditions and a different number of touch fingers. By establishing a lumped parameter thermal circuit model, the temperature of different nodes on the three-phase busbar of the switchgear is simulated.

In summary, the current research has analysed the electromagnetic-heat-flow field of the switchgear through simulation or experiment, but the thermal design of switchgear mainly focuses on the single measure of enhanced heat exchange. There are few kinds of research that focus on the combination of multiple heat exchange measures. Based on the three heat dissipation principles, including natural convection, forced convection and phase change, this paper studies the combination of three heat dissipation measures, including changing ventilation area, fan inlet flow rate and heat pipe, which optimises the thermal design of the busbar room of the switchgear through simulation, so as to further improve the power transmission capacity of switchgear.

2. Physical model and calculation method

Due to the complex arrangement of the busbar, the busbar room is usually the chamber with the highest temperature rise in the switchgear, and the KYN28A high voltage switchgear busbar room is taken as the research object in this paper.

2.1 Physical model and geometric parameters

The electromagnetic-heat-flow field coupling three-dimensional simulation model of the switchgear busbar room is established in this paper. Its physical model and geometric dimensions are shown in Figure 1. Its internal components include a three-phase busbar, contact box, tulip contact, moving contact and static contact. Some small components or structures in the model do not affect the flow and heat transfer inside the switchgear; they are omitted or simplified in the simulation.

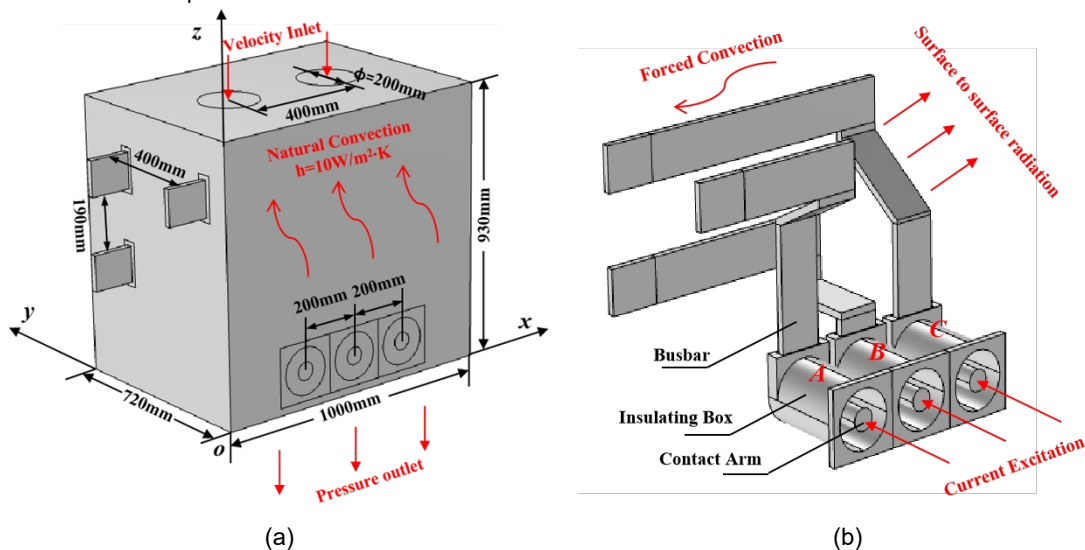


Figure 1: Physical model and geometric dimensions of switchgear busbar room: (a) external structure (b) internal structure

The cabinet surface of the busbar room is low alloy steel AISI 4340; The contact box is an insulating component made of epoxy resin which not only ensures the insulation performance but also has low thermal conductivity; The conductive circuit made of copper includes busbar and contact system; The contact surface between tulip contact and static contact is set with silver plating. The gas inside the cabinet, the contact box and the tulip contacts are all set as air whose physical parameters are the function of temperature.

2.2 Control equations and calculation methods

When the high-voltage switchgear is excited by the rated current, the conductive circuit generates Joule heat. The electromagnetic-heat coupling equations of the conductive circuit are as follows. The physical quantity of electric field is obtained by solving the current conservation equation Eq(1), Ohm's Law Eq(2) and electric field

intensity Eq(3). The electromagnetic loss obtained by the loss Eq(4) is applied to the heat conduction Eq(5) as a heat source.

$$\nabla \cdot \mathbf{J} = Q_{j,v} \quad (1)$$

$$\mathbf{J} = \sigma \mathbf{E} + j\omega \mathbf{D} + \mathbf{J}_e \quad (2)$$

$$\mathbf{E} = -\nabla V \quad (3)$$

$$Q_e = Q_{rh} = \frac{1}{2} \text{Re}(\vec{\mathbf{J}} \cdot \vec{\mathbf{E}}^*) \quad (4)$$

$$\rho C_p \vec{\mathbf{u}} \cdot \nabla T = \nabla \cdot (k \nabla T) + Q_e \quad (5)$$

where \mathbf{J} is the current density, A/m²; $Q_{j,v}$ is the Current source volume, A/m³, σ is the conductivity, S/m; \mathbf{E} is the electric field intensity, V/m; j is the imaginary unit; $\omega = 2\pi f$ is the phase angle, rad/s; $f = 50$ Hz is the excitation current frequency; \mathbf{D} is the electric flux density, C/m²; \mathbf{J}_e is the external current density, A/m²; V is the potential, V; Q_e is the electromagnetic loss, W/m³; Q_{rh} is resistance loss, W/m³; Q_{ml} is electromagnetic loss, W/ m³; $\vec{\mathbf{J}}$ is the current density vector, A/m²; $\vec{\mathbf{E}}^*$ is the electric field intensity vector, V/m; $\vec{\mathbf{B}}$ is the magnetic induction vector, T; $\vec{\mathbf{H}}^*$ is the magnetic field intensity vector, A/m²; Re is the real part of the imaginary number; ρ is the density, kg/m³; C_p is the constant pressure heat capacity, J/(kg·K); $\vec{\mathbf{u}}$ is the velocity vector, m/s; T is the temperature, K; k is the thermal conductivity, W/(m·K);

For the flow and heat transfer in the high-voltage switchgear, the continuity equation Eq(6), momentum equation Eq(7) and energy equation Eq(8) are as follows:

$$\rho(T) \nabla \vec{\mathbf{u}} = 0 \quad (6)$$

$$\rho(T) (\vec{\mathbf{u}} \cdot \nabla \vec{\mathbf{u}}) = -\nabla p + \nabla [(\mu(T) + \mu_T) (\nabla \vec{\mathbf{u}} + (\nabla \vec{\mathbf{u}})^T)] \quad (7)$$

$$\rho(T) (\vec{\mathbf{u}} \cdot \nabla T) = \nabla \cdot \left[\left(\frac{\lambda(T)}{C_p(T)} + \frac{\mu_T}{\sigma_T} \right) (\nabla T) \right] \quad (8)$$

where p is the pressure, Pa; $\mu(T)$ is the dynamic viscosity of air, Pa·s; $\lambda(T)$ is the thermal conductivity of air, W/(m·K); $C_p(T)$ is the constant pressure heat capacity of air, J/(kg·K); The physical properties of air are all functions of temperature; μ_T is turbulence viscosity of air, kg/(m·s); σ_T is the plant constant.

The radiation heat transfer exists between the inner surface of the switchgear enclosure and the outer surface of the conductors circuit. The radiation emissivity of the inner surface of the switchgear is $\varepsilon_k = 0.23$, and the radiation emissivity of the outer surface of the conductor circuit is $\varepsilon_c = 0.5$; The cross-section boundary of moving contact is the adiabatic boundary condition; The heat transfer of the external surface of the switchgear can be considered as natural convection outside vertical and horizontal plates, and the third boundary condition is adopted, $h = 10$ W/(m²·K), the ambient temperature is $T_{\text{sur}} = 303.15$ K.

In this study, the coupling multi-physical fields of the switchgear busbar room are solved by the finite element analysis software Comsol Multiphysics, the GMRES solver is used to solve the flow and heat transfer equation, and the BiCGSTAB solver is used to solve the electromagnetic field equation. When the calculated residual is less than 10^{-3} , the calculation is considered to have reached convergence.

3. Grid independence test and model validations

Firstly, the independence of the computational grid of the model is verified. In the current research, four groups of grids are tested, and the total numbers of these grids are 141,750, 267,927, 506,383 and 829,666. The highest temperature and electromagnetic loss density under steady-state are taken as the assessment indexes. The results show that when the total number of grids is 506,383, the calculation reaches the grid-independent solution, so this paper adopted a grid division method with the grids number of 506,383 for subsequent calculations.

In order to ensure the accuracy of the simulation, it is necessary to verify the calculation model and method. The temperature rise experiment of switchgear carried out by Li J.T. et al. (2019) is compared with the simulation results in this paper. The maximum relative errors of the temperature of phase A, phase B and phase C are 1.01 %, 2.42 % and 3.17 %. The results show that the experimental results are consistent with the simulation results. It can be proved that the calculation model and method used in this paper are reliable.

4. Results and discussion

In this study, the three heat dissipation measures, including changing the effective ventilation area, fans inlet flow rate and heat pipe, are studied. The specific combination configuration is set as shown in Table 1 below. From variant 1 to variant 4, the influence of effective ventilation area on natural convection is studied by changing the ventilation area at the top and bottom (modification 1 and modification 3); From variant 5 to variant 6, the influence of forced convection on the temperature rise of switchgear is studied by setting different groups of fans and their inlet flow velocity (modification 2); In variant 7, the temperature rise of contact system is improved by inserting a heat pipe for each phase (modification 4). After Setting the rated current to 4,000 A, the lap joint of the tulip contact and the static contact is taken as the starting point, and then the temperature contribution along with the B phase conductive circuit is studied.

Table 1: Thermal design configuration of switchgear busbar room

Variant name	Top cover	Layout	A_{in} (m ²)	A_{out} (m ²)	Area ratio	Heat pipe
Variant 1	Solid roof	Mod.1, Mod.3	0.0314	0.1194	3.8	-
Variant 2	Solid roof	Mod.1, Mod.3	0.0314	0.2388	7.6	-
Variant 3	Solid roof	Mod.1, Mod.3	0.0628	0.1194	1.9	-
Variant 4	Solid roof	Mod.1, Mod.3	0.0628	0.2388	3.8	-
Variant 5	Ventilated roof	Mod.1, Mod.2	0.0314	0.1194	3.8	-
Variant 6	Ventilated roof	Mod.1, Mod.2	0.0628	0.1194	1.9	-
Variant 7	Ventilated roof	Mod.2, Mod.4	0.0628	0.1194	1.9	Included

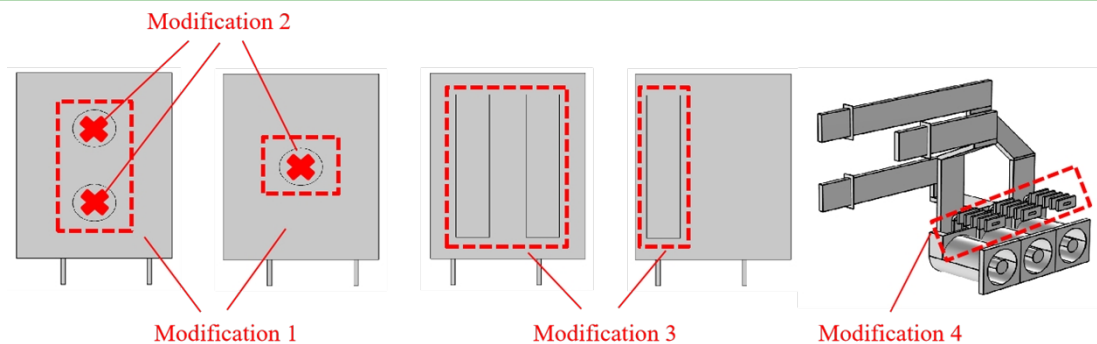


Figure 2: Thermal design of switch cabinet bus room: (Modification. 1) Top ventilation area; (Modification. 2) Inlet flow velocity; (Modification. 3) Bottom ventilation area; (Modification. 4) Heat pipe

The research results of variants 1-4 show that the temperature rise of the conductive circuit does not meet the IEEE standard under the four variants, so only natural convection cannot meet the demand of increasing the current carrying capacity of switchgear. The larger the ventilation area at the bottom, the lower the average temperature of the conductive circuit, and the maximum drop can reach 1.5 °C.

The research results of variants 5-6 are shown in Figure 3-Figure 4. With the increase in inlet flow rate, the overall temperature of the conductive circuit gradually decreases. In order to meet the IEEE standard and save energy consumption, the optimal working flow rate of variant 5 is 2 m/s, and that of variant 6 is 1.5 m/s. At the same flow rate, the average temperature of the conductive circuit in variant 6 is 2.4 °C lower than that in variant 5. However, due to the sealing effect of the contact box and the large Joule heat generated by the contact resistance at the contact lap, the cooling effect of the fan on the contact system is limited. When the inlet flow rate is less than 1.5 m/s, the temperature rise of the contact under both variants does not meet the IEEE standard. If the heat of the contact system can be conducted outside the contact box in time, the heat dissipation effect of the fan can be brought into better play.

The research results of variant 7 are shown in Figures 5 to 8. As shown in Figure 5, in the case of natural convection, after installing the heat pipe, the average temperature of the conductive circuit is reduced by 4.9 °C, the average temperature of the static contact is reduced by 7.2 °C, and the average temperature of the busbar is reduced by 4.7 °C. Due to the indirect heating of the busbar by the heat derived from the contact system by the heat pipe, the temperature decrease amplitude of the busbar is lower. Since the heat transmitted by the heat pipe cannot be dissipated in time, it is necessary to combine the heat pipe with the fan. As shown in Figure 6, after turning on the fan, the temperature of the contact system is lower than that of variant 6. With the increase

of fan inlet flow, the combination of the heat pipe and fan can significantly improve the heat dissipation of the contact system. Compared with variant 6, when the inlet velocity reaches 0.5 m/s, the average temperature of the conductive circuit decreases by 6.2 °C, and the average temperature of the static contact decreases by 9.5 °C; When it continues to increase to 1 m/s, the average temperature of the conductive circuit decreases by 9.7 °C, and the average temperature of the static contact decreases by 15.7 °C. As shown in Figures 7 and 8, the maximum temperature rise occurs at the contact of the C phase, reaching 85.7 °C. The vortex above phase A and phase B strengthens the exchange of cold and hot air near the heat pipe, so the temperature rise of phase C is relatively high.

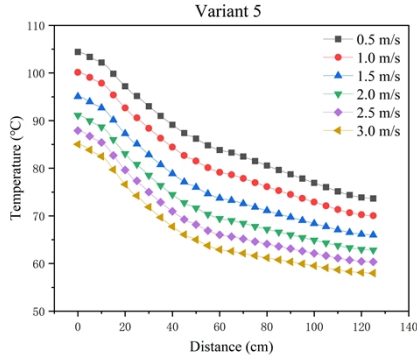


Figure 3: Temperature distribution of Variant 5

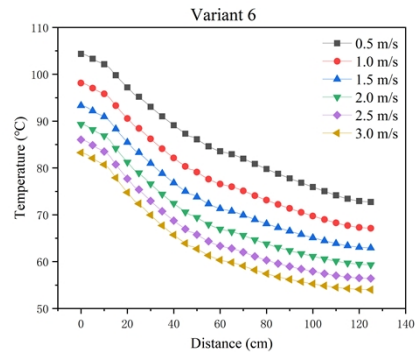


Figure 4: Temperature distribution of Variant 6

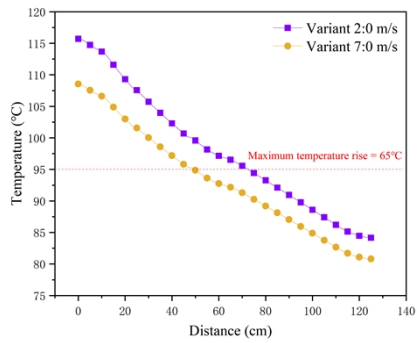


Figure 5: Temperature distribution of Variant 7 (Natural convection)

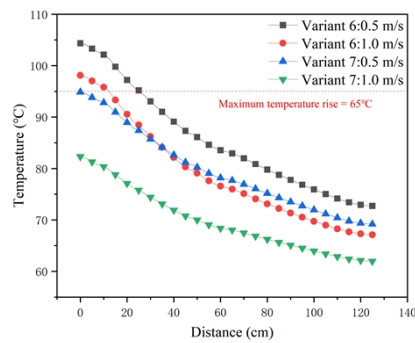


Figure 6: Temperature distribution of Variant 7 (Force convection)

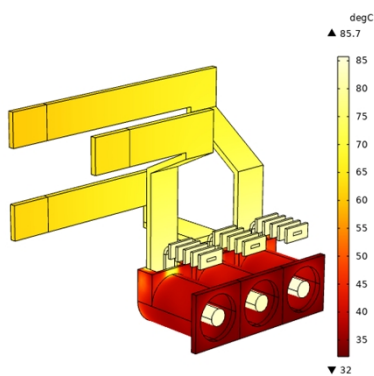


Figure 7: Temperature distribution of Variant 7: 1m/s

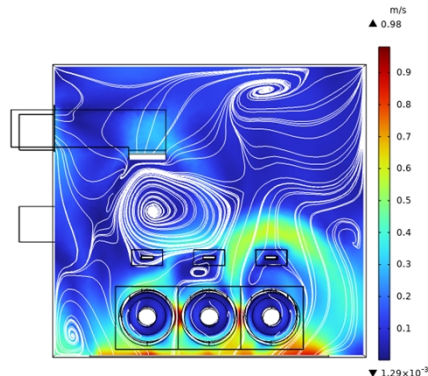


Figure 8: Velocity distribution of Variant 7: 1m/s

5. Conclusions

The thermal design is carried out for the busbar room of the switchgear to solve the overheating problem. The main conclusions are as follows:

- (1) The influence of the bottom ventilation area is greater than that of the top ventilation area under natural convection.
- (2) In order to meet the IEEE standard and save energy consumption, the optimal working flow rate of a single group of the fan is 1.5 m/s, and that of double groups of the fan is 2 m/s.
- (3) The combination of fan and heat pipe can effectively solve excessive local temperature rise of the contact system. When the inlet flow rate is 1 m/s, the average temperature of the phase B circuit and static contact decreased by 9.7 °C and 15.7 °C.

The research of this paper strengthens the heat dissipation performance of the switchgear busbar room, which can further increase the current carrying capacity of the switchgear from 3,000 A to 4,000 A.

Acknowledgements

This work was supported by the S&T project of State Grid Corporation of China under grant number 52094020004H.

References

- Bedkowski, M., Smolka J., Bulinski Z., Ryfa A., 2016, 2.5-D multilayer optimisation of an industrial switchgear busbar system, *Applied Thermal Engineering*, 101, 147-155.
- Bedkowski, M., Smolka J., Bulinski Z., Ryfa A., 2017, Simulation of cooling enhancement in industrial low-voltage switchgear using validated coupled CFD-EMAG model, *International Journal of Thermal Sciences*, 111, 437-449.
- Guan X.Y., Shu N.Q., Kang B., Zou M.H., 2015, Multiphysics analysis of plug-in connector under steady and short circuit conditions, *IEEE Transactions on Components, Packaging and Manufacturing Technology*, 5, 320-327.
- IEEE Draft Standard for Metal-Clad Switchgear, 2022, IEEE PC37.20.2/D17, 2022, 1-92.
- Jia X.Y., Si W.R., Fu C.Z., Wu Y.N., Wang Q.W., Lin M., Yang J., 2020, Multi-physics coupling simulation of heat transfer in transformer winding, *Chemical Engineering Transactions*, 81, 337-342.
- Li J.T., Sun Y., Ning D., Zhao Z., 2019, A novel contact temperature calculation algorithm in distribution switchgears for condition assessment, *IEEE Transactions on Components, Packaging and Manufacturing Technology*, 9, 279-287.
- Liu G.T., Zhong R.F., 2018, Experimental study on capacity increase of 12 kV switchgear based on pumpless self-circulation evaporative cooling technology, 2018 International Conference on Power System Technology (POWERCON), Guangzhou, China, 6-8 Nov., 3105-3111.
- Ruan J.J., Wu Y.C., Li P., Long M.Y., Gong Y.J., 2019, Optimum methods of thermal-fluid numerical simulation for switchgear, *IEEE Access*, 7, 32735-32744.
- Szulborski M., Apczyński S., Kolimas U., 2021, Thermal analysis of heat distribution in busbars during rated current flow in low-voltage industrial switchgear, *Energies*, 14, 1-23.
- Wang X.R., Xia H.T., Yu Z.Q., Guan Y.G., Zhao B., Huang Y.L., Qu L., Ding J.D., 2020, Precise multi-dimensional temperature-rise characterization of switchgear based on multi-conditional experiments and LPTN model for high-capacity application, *High Voltage*, 6, 138-148.
- Wang Z.B., Wang R., Yao C.W., Ma X.Y., Sun S., Wang L.J., 2021, Simulation study on the influence of forced convection heat dissipation on the temperature rise of switchgear, *High Voltage Engineering*, 47, 1064-1074.